AMSE Association for the Advancement of Modelling & Simulation Techniques in Enterprises
IIETA International Information and Engineering Technology Association
Advancing the World of Information and Engineering

Advances in Modelling and Analysis C
Vol. 73, No. 4, December, 2018, pp. 150-157
Journal homepage: http://iieta.org/Journals/AMA/AMA_C

Sliding mode control based on backstepping approach for a double star induction motor (DSIM)

H. Rahali[1*], S. Zeghlache[2], L. Benalia[3], N. Layadi[1]

[1] Electrical Engineering lab., Department of Electrical Engineering, Faculty of Technology, University Mohamed Boudiaf of M'sila, BP 166, Ichbilia 28000, Algeria
[2] Signal and Systems Analysis Lab., Department of Electrical Engineering, Faculty of Technology, University Mohamed Boudiaf of M'sila, BP 166, Ichbilia 28000, Algeria,
[3] Electrical Engineering Lab., Department of Electrical Engineering, Batna-2 University, Street Chahid Med El Hadi boukhlouf, Algeria

Corresponding Author Email: hilal_lami@yahoo.fr

https://doi.org/10.18280/ama_c.730404

Received: 11 June 2018
Accepted: 15 October 2018

Keywords:
sliding mode, speed control, backstepping, DSIM, chattering

ABSTRACT

This paper proposes a sliding mode controller based on backstepping approach, to control the speed of a dual star induction machine (DSIM), to get best performances of the system. A control strategy based on the coupling of these two methods (Backstepping and sliding mode controllers) are used to guaranteeing the stability and the robustness of the machine and to force the rotor angular speed to follow a desired reference signal. The simulations results obtained from MatLab/Simulink of the proposed controller are finally presented and discussed; the obtained results show that the controller can greatly alleviate the chattering effect, in enhancing the robustness of control systems with high accuracy.

1. INTRODUCTION

The dual star induction machine (DSIM) is the more used as motor or generator particularly in autonomous system [1], each series of three-phase windings is usually fed by a three-phase voltage source inverter for the variation of speed [2, 3, 4], this type of multi-phase machine habitually with a squirrel cage rotor [5]. DSIM is very often treated in the literature in reason of its several advantages, such as: lower torque ripple, speed and torque capacity, reliability, high power, higher efficiency, decreases rotor harmonic currents, less dc-link current harmonics [3-7], one important advantage compared to the classic three phases system is its large fault-tolerance in reason to the large number of phases they possess [5]. The DSIM is used in applications requiring high power such as electric vehicles, locomotive traction, and naval applications [4, 6, 7].

DSIM is economic and doesn't need maintenance because is magnet-less and brushless [5]. The maximum decrease of torque pulsations is obtained in case the two three-phase stator winding series are shifted by $\pi/6$ electrical radians [8]. The multi-phase induction motor can continue to function even with open-phase faults because the fundamental component of the air-gap magnetic field is retained, this fault tolerance without additive hardware increasing the use of multi-phase machine and become very important especially in systems that requires safety conditions as the field of aerospace, in offshore wind energy systems where the troubleshooting depends on weather and in traction applications [9].

Recently, the Sliding mode control of nonlinear systems remains an important area of research in the field of machine control. Like this, considerable efforts and different works are carried out in the sliding mode, namely a sliding mode control (SMC) associated to the field oriented control (FOC) of a dual-stator induction generator (DSIG) based wind energy conversion systems (WECSs) [10], the fault tolerant control (FTC) of the induction motor (IM) in order to improve its performances under faulty state, starting from [11].

In the last few years, few researches proposed another control methods for application on the DSIM to improve its performances starting from [7], where the speed reference tracking is examined for two double star induction motors connected in parallel to a single six-phase inverter supply. In that papers authors make a comparative study between two control structures, indirect field oriented control (IFOC) using fuzzy logic controller (FLC) based only on four rules and IFOC with classic proportional integral (PI). Each control method is applied on one DSIM. In the first method, FLC which does not need an accurate mathematical model of the system ensures high performance in speed response under different operating conditions more than PI controller. In [3] another comparative analysis between the two IFOC using traditional PI and FLC, the both control design are applied on DSIM under load torque and rotor resistance variations, the simulation results shows clearly the robustness of the FLC approach because the development of this intelligent control does not depend on parameters variations. In [4] a DSIM under load disturbances and parameter variations (rotor resistance, inertia moment) is inspected. The IFOC using FLC apply on DSIM shows robustness against parameter variations and guarantee a good performance in transient regime and steady state more than IFOC using classic PI. A fault tolerant control (FTC) operation of DSIM has been recently analyzed starting from [2].

To prove the efficiency and robustness satisfactory of the sliding mode controller based on backstepping approach, a comparative study between the strategy of the proposed

control and the rotor flux oriented control (RFOC) accompanied by simulation results and analysis.

The principal contribution of this paper is to develop a control technique based on the development and the synthesis of a control algorithm based upon sliding mode based on backstepping approach ensuring the locally asymptotic stability.

This paper is organized as follow in section 2 a description and modeling of DSIM. In section 3 a sliding mode control based on backstepping approach is designed for the DSIM which assures to steer the speed and flux to their desired references and reject the effect of speed variation (inversion), during this section the stability of the closed loop system is verified by Lyapunov stability theory. Some simulation results and their interpretation are given in section 4. The last section is reserved for conclusion.

2. DESCRIPTION AND MODELING OF DSIIM

The windings of the dual star induction machine are represented in figure 1, the DSIM is composed by two stars separate with three phases winding fixed and standard simple squirrel-cage rotor composed three rotors phases moving. The two stators is displaced by angle ($\alpha=\pi/6$), their axes are shifted from each other an electrical angle equal to ($2\pi/3$) with isolated neutrals [10, 12-13]. Therefore, the orthogonality created between the two oriented fluxes, which must be strictly observed, leads to generate decoupled control with an optimal torque [14, 15].

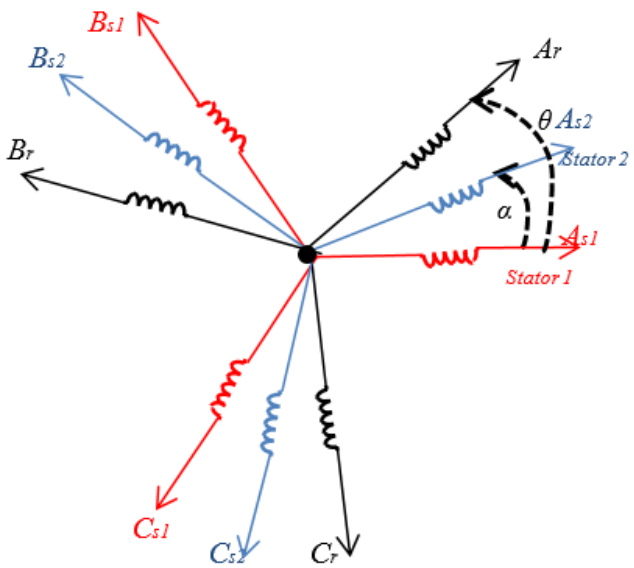

Figure 1. Representation of the DSIM winding

2.1 DSIM model

The Park model of DSIM in a (d-q) rotating frame is presented below.

Electrical equations used to model of the DSIM given by:

$$\begin{cases} V_{ds1} = R_{s1} i_{ds1} + \dfrac{d}{dt}\varphi_{ds1} - \omega_s \varphi_{qs1} \\ V_{qs1} = R_{s1} i_{qs1} + \dfrac{d}{dt}\varphi_{qs1} + \omega_s \varphi_{ds1} \\ V_{ds2} = R_{s2} i_{ds2} + \dfrac{d}{dt}\varphi_{ds2} - \omega_s \varphi_{qs2} \\ V_{qs2} = R_{s2} i_{qs2} + \dfrac{d}{dt}\varphi_{qs2} + \omega_s \varphi_{ds2} \\ 0 = R_r i_{dr} + \dfrac{d}{dt}\varphi_{dr} + (\omega_s - \omega_r)\varphi_{qr} \\ 0 = R_r i_{qr} + \dfrac{d}{dt}\varphi_{qr} + (\omega_s - \omega_r)\varphi_{dr} \end{cases} \quad (1)$$

Expression of the electromagnetic torque of DSIM is given by:

$$C_{em} = p\frac{L_m}{L_m + L_r}\left[\varphi_{dr}\left(i_{qs1} + i_{qs2}\right) - \varphi_{qr}\left(i_{ds1} + i_{ds2}\right)\right] \quad (2)$$

In field oriented control, the flux vector is forced to align with the d-axis (ϕ_q =0) in order to have decoupling model which is similar to a DC motor. The system of state equation of the DSIM in the reference (d, q) is given by Eq. (3):

$$\begin{cases} \dot{i}_{ds1} = \dfrac{1}{L_{s1}}(V_{ds1} - R_{s1} i_{ds1} + \omega_s (L_{s1} i_{qs1} + \mathrm{T}_r \phi_{rref} \omega_{glref})) \\ \dot{i}_{qs1} = \dfrac{1}{L_{s1}}(V_{qs1} - R_{s1} i_{qs1} - \omega_s (L_{s1} i_{ds1} + \phi_{rref})) \\ \dot{i}_{ds2} = \dfrac{1}{L_{s2}}(V_{ds2} - R_{s2} i_{ds2} + \omega_s (L_{s2} i_{qs2} + \mathrm{T}_r \phi_{rref} \omega_{glref})) \\ \dot{i}_{qs2} = \dfrac{1}{L_{s2}}(V_{qs2} - R_{s2} i_{qs2} - \omega_s (L_{s2} i_{ds2} + \phi_{rref})) \\ \dot{\Omega} = \dfrac{1}{j}(p\dfrac{L_m}{L_m + L_r}\phi_{rref}(i_{qs1} + i_{qs2}) - C_r - K_f \Omega) \\ \dot{\phi}_r = \dfrac{-\mathrm{R}_r}{L_m + L_r}\phi_r + \dfrac{L_m . \mathrm{R}_r}{L_m + L_r}(i_{ds1} - i_{ds2}) \end{cases} \quad (3)$$

The field oriented control (FOC) of with a conventional PI speed controller is required in principle by some industrial processes. It is easy to design and implement, but it has difficulty in dealing with parameter variations, and load disturbances [14, 16].

With the problems posed, the PI controllers lose their performance and should be badly regulated, to overcome these problems, a robust control strategy based on synthesis of the hybrid backstepping and sliding mode to control speed and flux of the double star induction machine.

3. SLIDING MODE CONTROL BASED ON BACKSTEPPING APPROACH

The Sliding Mode Control (SCM) is an effective control strategy in modern control because of its robustness and simple realization, it is consists in bringing the state trajectory of a system towards a chosen manifold in the state space, called the sliding surface and making it switch by means of a suitable switching logic around it to the equilibrium point [17].

A problem of the conventional sliding mode controller technique is produces high frequency oscillations and dangerous vibrations in its outputs called chattering. Chattering is undesirable in conventional sliding mode controller in practice, because it can excite the high frequency dynamics of the system. In order to guarantee the performance, stability and robustness of the sliding mode controller to the uncertainties it has eliminated the chattering.

The basic idea of the backstepping control (BSC) design is that can effectively linearize a non linear system such as DSIM in the presence of uncertainties. The BSC decompose the global law of control, by dividing the Backstepping design into various design steps using the intermediate control (virtual control) result in each step deals with a single input–single-output design problem, and each step as reference signal for the next design step until completion of the control design (actual control). The objective of the controller is to build an adequate function of Lyapunov guaranteed that the system is asymptotically stable and to achieve the objectives tracking.

The recursive nature of the proposed control design is similar to the standard backstepping methodology. However, the proposed control design uses backstepping to design virtual controllers with a zero-order sliding surface at each recursive step. The benefit of this approach is that each virtual controller can compensate for unknown bounded function which contains unmodelled dynamics and external disturbances [18].

The choice of this method is not fortuitous considering the major advantages it presents [19]:

− It ensures Lyapunov stability.

− It ensures the robustness and all properties of the desired dynamics.

− It ensures the handling of all system nonlinearities.

The block diagram of the sliding mode control based on backstepping approach is shown in Figure 2; it contains an equivalent control part and discontinues control.

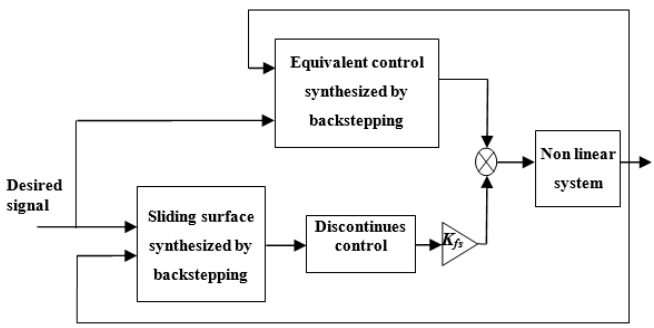

Figure 2. Diagram of the equivalent control part and discontinues control

Sliding mode control based on backstepping approach for a double star induction motor can be achieved in two successive steps. The bloc diagram of the proposed controller is shown in Figure 3.

Step 1: Speed and Flux regulators

The sliding surface requires to as to retain, so the error on the sliding surface s (e, t) =0, if for that which brings back us to define the speed equivalent control and the rotor flux module in the following way:

$$\dot{s} = \begin{cases} S_w = 0 \\ S_\varphi = 0 \end{cases} \tag{4}$$

The rotor speed and the rotor flux surface S_ω and S_ϕ are defined by:

$$\begin{cases} S_w = \omega_{ref} - \omega_r \\ S_\varphi = \phi_{ref} - \phi_r \end{cases} \tag{5}$$

Derivative of the sliding surface S_ω and S_φ are calculated by:

$$\begin{cases} \dot{S}_\omega = \dot{\omega}_{rref} - \dot{\omega}_r \\ \dot{S}_\phi = \dot{\phi}_{rref} - \dot{\phi}_r \end{cases} \tag{6}$$

Replacing the derivate of the speed ω_r and flux ϕ from Eq. (3) in Eq. (6), thus one obtains the following equations:

$$\dot{S}_\omega = \dot{\omega}_{rref} - \frac{p^2}{j}\frac{L_m}{L_m + L_r}\phi_{rref}(i_{qs1} + i_{qs2}) + C_r\frac{p}{j} + \frac{K_f}{j}\omega_r \tag{7}$$

$$\dot{S}_\phi = \dot{\phi}_{rref} + \frac{R_r}{L_m + L_r}\phi_r - \frac{R_r L_m}{L_m + L_r}(i_{ds1} + i_{ds2}) \tag{8}$$

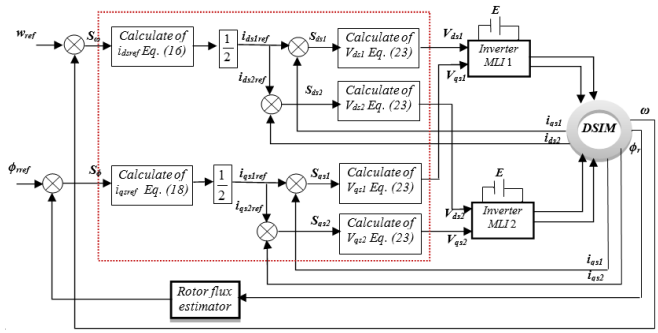

Figure 3. Diagram of the sliding mode control based on backstepping approach

We define the first function of Lyapunov V_1 which constitutes the speed and flux sliding surface as follows by:

$$V_1 = \frac{1}{2}(S_\omega^2 + S_\phi^2) \tag{9}$$

The time derivative of Eq. (9) is obtained by:

$$\dot{V}_1 = S_\omega \dot{S}_\omega + S_\phi \dot{S}_\phi \tag{10}$$

Accounting Eq. (7) and Eq. (8), one can rewrite Eq. (10) as follows:

$$\dot{V}_1 = S_\omega \left\{ \begin{array}{l} \dot{\omega}_{rref} - \dfrac{p^2}{j} \dfrac{L_m}{L_m + L_r} \phi_{rref} (i_{qs1} + i_{qs2}) \\ + C_r \dfrac{p}{j} + \dfrac{K_f}{j} \omega_r \end{array} \right\} + S_\phi \left\{ \dot{\phi}_{rref} + \frac{R_r}{L_m + L_r} \phi_r - \frac{R_r L_m}{L_m + L_r} (i_{ds1} + i_{ds2}) \right\} \tag{11}$$

The chosen low for the attractive surface of Eq. (11) stratifying the necessary condition of sliding $(s_i.\dot{s}_i) < 0$ is given by:

$$\dot{s}_i = -K_{fsi} \tanh(s_i) \tag{12}$$

According to the required sliding condition obtained in Eq. (12) we propose:

$$\dot{\omega}_{rref} - \frac{p^2}{j} \frac{L_m}{L_m + L_r} \phi_{rref} (i_{qs1} + i_{qs2}) + C_r \frac{p}{j} + \frac{K_f}{j} \omega_r = -K_{fs\omega} \tanh(S_\omega) \tag{13}$$

$$\dot{\phi}_{rref} + \frac{R_r}{L_m + L_r} \phi_r - \frac{R_r L_m}{L_m + L_r} (i_{ds1} + i_{ds2}) = -K_{fs\phi} \tanh(S_\phi) \tag{14}$$

Assuming that: $i_{ds1ref} + i_{ds2ref} = 2 i_{ds1ref} = i_{dsref}$ So $i_{ds1ref} = i_{ds2ref} = \frac{1}{2} i_{dsref}$

$$\dot{\phi}_{rref} + \frac{R_r}{L_m + L_r} \phi_r + K_{fs\phi} T2FLC(S_\phi) = \frac{R_r L_m}{L_m + L_r} i_{dsref} \tag{15}$$

Finally, the reference current i_{ds} is determinate from the following expression:

$$i_{dsref} = (\dot{\phi}_{rref} + \frac{R_r}{L_m + L_r} \phi_r + K_{fs\phi} \tanh(S_\phi)) \frac{L_m + L_r}{R_r L_m} \tag{16}$$

Similar to the I_{dsref1} case; the Eq. (13) becomes:

$$\dot{\omega}_{rref} + C_r \frac{p}{j} + \frac{K_f}{j} \omega_r + K_{fs\omega} \tanh(S_\omega) = \frac{p^2}{j} \frac{L_m}{L_m + L_r} \phi_{rref} i_{qsref} \tag{17}$$

The reference current i_{qs} is determinate by the following expression:

$$i_{qsref} = (\dot{\omega}_{rref} + C_r \frac{p}{j} + \frac{K_f}{j} \omega_r + K_{fs\omega} \tanh(S_\omega)) \frac{j}{p^2} \frac{L_m + L_r}{L_m \phi_{rref}} \tag{18}$$

Step 2: Currents regulators

In this step four new errors of the components of the stator current given by:

$$\left\{ \begin{array}{l} S_{ds1} = i_{ds1ref} - i_{ds1} \\ S_{ds2} = i_{ds2ref} - i_{ds2} \\ S_{qs1} = i_{qs1ref} - i_{qs1} \\ S_{qs2} = i_{qs2ref} - i_{qs2} \end{array} \right. \tag{19}$$

The augmented Lyapunov function for the second step is given by:

$$V_2 = \frac{1}{2} (S_\omega^2 + S_\phi^2 + S_{ds1}^2 + S_{ds2}^2 + S_{qs1}^2 + S_{qs2}^2) \tag{20}$$

We take note that V_2 is chosen in such a way that permit achieving control law.

The derivative of the positive definite function V_2 is:

$$\dot{V}_2 = S_\omega \dot{S}_\omega + S_\phi \dot{S}_\phi + S_{ds1} \dot{S}_{ds1} + S_{ds2} \dot{S}_{ds2} + S_{qs1} \dot{S}_{qs1} + S_{qs2} \dot{S}_{qs2} \tag{21}$$

By applying the Lyapunov stability theorem as in the first step, we obtain:

$$\left\{ \begin{array}{l} \dot{S}_{ds1} = \dot{i}_{ds1ref} - \dfrac{1}{L_{s1}} \{ V_{ds1} - R_{s1} i_{ds1} + \omega_s (L_{s1} i_{qs1} + T_r \phi_{rref} \omega_{glref}) \} \\ \dot{S}_{ds2} = \dot{i}_{ds2ref} - \dfrac{1}{L_{s2}} \{ V_{ds2} - R_{s2} i_{ds2} + \omega_s (L_{s2} i_{qs2} + T_r \phi_{rref} \omega_{glref}) \} \\ \dot{S}_{qs1} = \dot{i}_{qs1ref} - \dfrac{1}{L_{s1}} \{ V_{qs1} - R_{s1} i_{qs1} - \omega_s (L_{s1} i_{ds1} + \phi_{rref}) \} \\ \dot{S}_{qs2} = \dot{i}_{qs2ref} - \dfrac{1}{L_{s2}} \{ V_{qs2} - R_{s2} i_{qs2} - \omega_s (L_{s2} i_{ds2} + \phi_{rref}) \} \end{array} \right. \tag{22}$$

Finally, by putting equivalence between system of Eq. (22) and Eq. (12), we obtain Eq. (23) who is represented the real control.

$$\begin{cases} V_{ds1} = L_{s1}(K_{fsds1}\tanh(S_{ds1}) + \dot{i}_{ds1ref}) - \\ R_{s1}i_{ds1} + \omega_s(L_{s1}i_{qs1} + T_r\phi_{rref}\omega_{glref}) \\ V_{ds2} = L_{s2}(K_{fsds2}\tanh(S_{ds2}) + \dot{i}_{ds2ref}) - \\ R_{s2}i_{ds2} + \omega_s(L_{s2}i_{qs2} + T_r\phi_{rref}\omega_{glref}) \\ V_{qs1} = L_{s1}(K_{fsqs1}\tanh(S_{qs1}) + \dot{i}_{qs1ref}) - \\ R_{s1}i_{qs1} - \omega_s(L_{s1}i_{ds1} + \phi_{rref}) \\ V_{qs2} = L_{s2}(K_{fsqs2}\tanh(S_{qs2}) + \dot{i}_{qs2ref}) - \\ R_{s2}i_{qs2} - \omega_s(L_{s2}i_{ds2} + \phi_{rref}) \end{cases} \quad (23)$$

We can write equation Eq. (23) as follows:

$$\begin{aligned} \dot{V}_2 &= S_\omega(-K_\omega\tanh(S_\omega)) + S_\phi(-K_\phi\tanh(S_\phi)) + \\ &S_{ds1}(-K_{fsds1}T2\tanh(S_{ds1})) + \\ &S_{ds2}(-K_{fsds2}\tanh(S_{ds2})) + \\ &S_{qs1}(-K_{fsqs1}\tanh(S_{qs1})) + S_{qs2}(-K_{fsqs2}\tanh(S_{qs2})) \end{aligned} \quad (24)$$

The chosen low for the attractive surface of Eq. (21) stratifying the necessary condition of sliding $(s_i.\dot{s}_i) < 0$ obtained in Eq. (24):

$$\dot{s}_i = -K_{fsi}\tanh(s_i) \quad (25)$$

As for the sliding mode control based on backstepping approach, we must find a control law to reach it and stay thereafter:

$$u = u_{eq} + u_s \quad (26)$$

where u_{eq} is the equivalent control. It makes the derivative of the sliding surface equal to zero to stay on the sliding surface, us is the discontinuous control.

The condition to stay on the sliding surface is $\dot{s}_i = 0$; therefore, the equivalent control is:

$$\begin{cases} u_{eq\omega} = \frac{j}{p^2}\frac{L_m + L_r}{L_m\phi_{rref}}(\dot{\phi}_{rref} + \frac{R_r}{L_m + L_r}\phi_r) \\ u_{eq\phi} = \frac{L_m + L_r}{R_r L_m}(\dot{\omega}_{rref} + C_r\frac{p}{j} + \frac{K_f}{j}\omega_r) \\ u_{eqds1} = L_{s1}\dot{i}_{ds1ref} - R_{s1}i_{ds1} + \omega_s(L_{s1}i_{qs1} \\ +T_r\phi_{rref}\omega_{glref}) \\ u_{eqds2} = L_{s2}\dot{i}_{ds2ref} - R_{s2}i_{ds2} + \omega_s(L_{s2}i_{qs2} \\ +T_r\phi_{rref}\omega_{glref}) \\ u_{eqqs1} = L_{s1}\dot{i}_{qs1ref} - R_{s1}i_{qs1} - \omega_s(L_{s1}i_{ds1} + \phi_{rref}) \\ u_{eqqs2} = L_{s2}\dot{i}_{qs2ref} - R_{s2}i_{qs2} - \omega_s(L_{s2}i_{ds2} + \phi_{rref}) \end{cases} \quad (27)$$

At this present stage, the control discontinuous control law u_{si} is designed as:

$$\begin{cases} u_{s\omega} = \frac{j}{p^2}\frac{L_m + L_r}{L_m\phi_{rref}}(K_{fs\omega}\tanh(S_\omega)) \\ u_{s\phi} = \frac{L_m + L_r}{R_r L_m}(K_{fs\phi}\tanh(S_\phi)) \\ u_{sds1} = L_{s1}K_{fsds1}\tanh(S_{ds1}) \\ u_{sds2} = L_{s2}K_{fsds2}\tanh(S_{ds2}) \\ u_{sqs1} = L_{s1}K_{fsqs1}\tanh(S_{qs1}) \\ u_{sqs2} = L_{s1}K_{fsqs2}\tanh(S_{qs2}) \end{cases} \quad (28)$$

4. SIMULATION RESULTS

The proposed control strategy of the speed and flux regulation of 4.5 Kw dual stator induction machine designed in this work has been done and validated by Matlab and Simulink® software, whose parameters are given in Table 3 in Appendix B.

Following figures (4-7) shows the simulated responses of speed, rotor field, electromagnetic torque, and the d-q axis stator currents respectively.

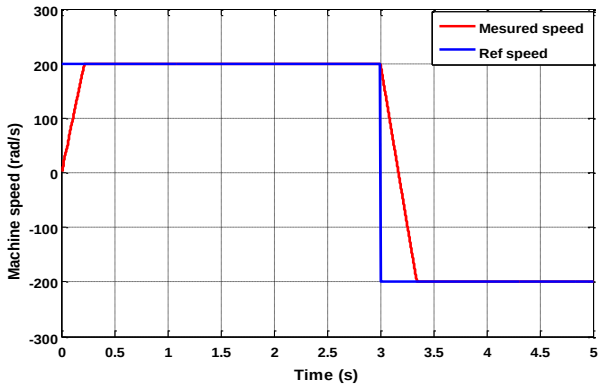

Figure 4. Simulated results of Speed response

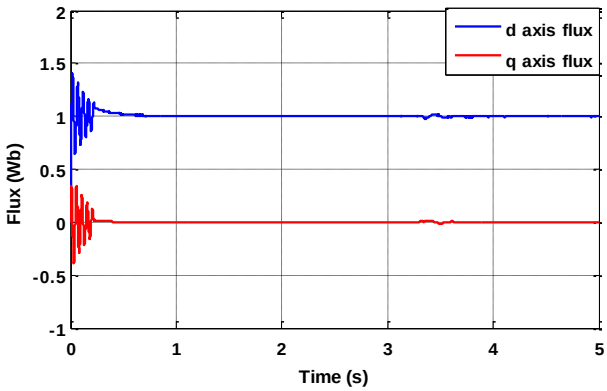

Figure 5. Simulated results of rotor flux

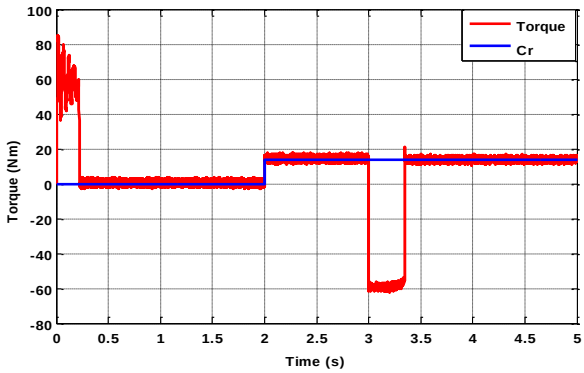

Figure 6. Simulated results of Torque under a load C_r=14 *N.m* in 2 *s*

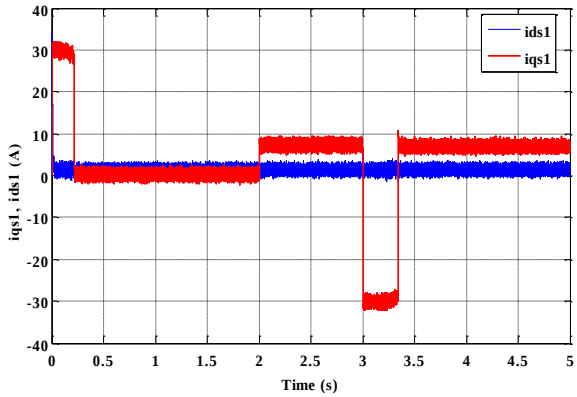

Figure 7. Simulated results of currents stator (i_{qs1}, i_{ds1}) under a load C_r=*14 N.m* in *2 s*

The initial rotation speed of the motor is 200 rd/s, to 3 sec up to -200 rd/s during a period of 0.3 s and after it is fixed a -200 rd/s, while the other parameters are held constant. The initial load torque of the motor 14 N.m is abruptly applied at 2 sec (Figure (5)), until the end and pursued by an inversion of speed reference between ± 200 rd/s at 3 s.

In figure (5), the decoupling of torque-flux is maintained in permanent mode.

The torque rises quickly when you the load disturbance torque increased from 0 to 14N.m (Figure (6)), this increase showing the effectiveness of the proposed control, who is rejects the load disturbance very rapidly, the other side the torque decreases quickly to attain the commanded value, once the speed degraded and reaches the value -200 rd/s, thereafter the torque settles to provide only the losses of the machine.

Figure (7) shows that the response of the current of the q axis which controls the torque is similar to that of the electromagnetic torque, whereas the current of the axis d which controls the flow of the rotor remains constant.

In order to compare the performance of the sliding mode controller based on backstepping approach with RFOC based on proportional-integral (PI) controller in the similar test, the Figures 8, 9 and 10 shows the simulated results comparison for the speed responses and currents stator (i_{qs1}; i_{ds1}) of conventional PI and the proposed controller.

Fig. 8.a shows the speed responses for the two control methods, in both controllers we clearly see that the speed responses follows its reference value with negligible overtake and without oscillations, but the response of speed of the sliding mode controller based on backstepping approach can handle the rapid change in load torque with a response time inferior a 0.2 sec, whereas the PI controller has the response is not as fast as compared to the proposed controller, she reached 0.4 sec.

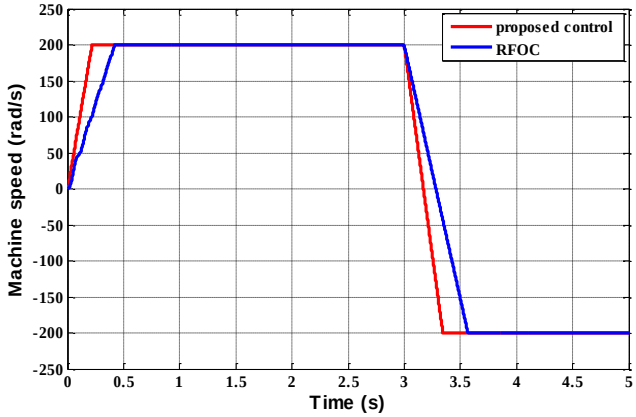

Figure 8. Simulated results of speed response of the proposed controller and FOC

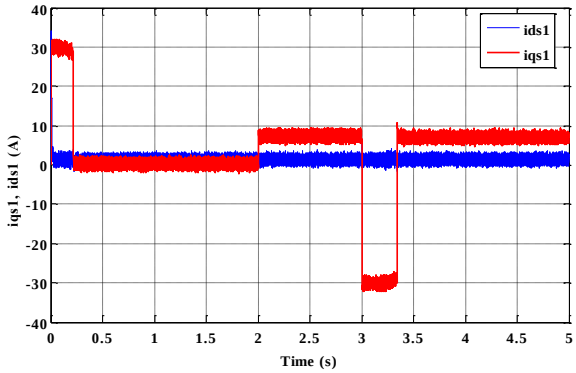

Figure 9. Simulated results of currents stator (i_{qs1}, i_{ds1}) under a load C_r=*14 N.m* in *2 s* of the proposed controller

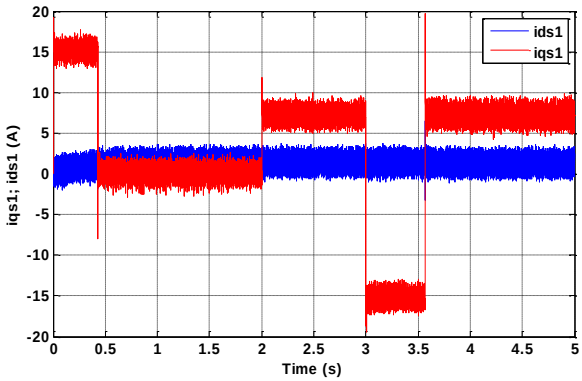

Figure 10. Simulated results of currents stator (i_{qs1}, i_{ds1}) under a load C_r=*14 N.m* in *2 s* of the FOC controller

It can be seen in Figures 09 and 10 show the behavior of the currents i_{qs}, i_{ds} of the first stator, the current i_q of the q axis controls the torque for the two control methods, but the obtained results summarize and reflect the response swiftness of our proposed controller compared to the RFOC.

Those results confirm the high performance of the proposed controller demonstrates robustness under various operating conditions and assure global stability of this machine.

5. CONCLUSION

This paper developed a hybrid non-linear control based on sliding mode controller and backstepping approach in order to make the error converges to zero and guaranteeing the stability and the robustness of the system.

The simulation results have confirmed the efficiency of the proposed controller and presented satisfactory dynamic performances, robust and assures global stability, it allows to have fast response without overtaking, settling time in speed response minimize and complete decoupling between the flux and the torque.

Finally; the experimental implementation of the proposed control scheme will be addressed in the future work.

REFERENCES

[1] Kouki H, Ben Fredj M, Rehaoulia H. (2015). SVPWM control strategy to minimize circulation harmonic currents for VSI fed double star induction machine. 12th International Multi-Conference on Systems. Signals & Devices SSD15: 1-7. https://doi.org/10.1109/SSD.2015.7348157

[2] Layadi N, Zeghlache S, Benslimane T, Berrabah F. (2017). Comparative analysis between the rotor flux oriented control and backstepping control of a double star induction machine (DSIM) under open-phase fault. AMSE Journals, Series Advances C 72(4): 292-311.

[3] Lekhchine S, Bahi T, Soufi Y. (2014). Indirect rotor field oriented control based on fuzzy logic controlled double star induction machine. International Journal of Electrical Power & Energy Systems 57: 206-211. https://doi.org/10.1016/j.ijepes.2013.11.053

[4] Tir Z, Soufi Y, Hashemnia MN. (2017). Fuzzy logic field oriented control of double star induction motor drive. Electrical Engineering 99: 495-503. https://doi.org/10.1007/s00202-016-0377-2

[5] Basak S, Chakraborty C. (2015). Dual stator winding induction machine: Problems, progress, and future scope. IEEE Transactions on Industrial Electronics 62(7): 4641-4652. https://doi.org/10.1109/tie.2015.2409800

[6] Wang C, Wang K, You X. (2016). Research on synchronized SVPWM strategies under low switching frequency for six-phase VSI-fed asymmetrical dual stator induction machine. IEEE Transactions on Industrial Electronics 63(11): 6767-6776. https://doi.org/10.1109/TIE.2016.2585459

[7] Tir Z, Malik OP, Eltamaly AM. (2016). Fuzzy logic based speed control of indirect field oriented controlled double star induction motors connected in parallel to a single six-phase inverter supply. Electric Power Systems Research 134: 126-133. https://doi.org/10.1016/j.epsr.2016.01.013

[8] Dainez PS, Bim E, Glose D. (2015). Modeling and parameter identification of a double-star induction machines. Electric Machines & Drives Conference, IEMDC 2015, Coeur d'Alene 749-755. https://doi.org/10.1109/IEMDC.2015.7409143

[9] Guzman H, Duran MJ, Barrero F. (2016). Comparative study of predictive and resonant controllers in fault-tolerant five-phase induction motor drives. IEEE Transactions on Industrial Electronics 63(1): 606-617. https://doi.org/10.1109/TIE.2015.2418732

[10] Lekhchine S, Bahi T, Soufi Y. (2014). Indirect rotor field oriented control based on fuzzy logic controlled double star induction machine. International Journal of Electrical Power & Energy Systems 57: 206-211. https://doi.org/10.1016/j.ijepes.2013.11.053

[11] Belhamdi Saad S, Goléa A. (2011). Sliding mode control of asynchronous machine presenting defective rotor bars. AMSE Journals, Series Advances C 66(1/2): 39-49.

[12] Tir Z, Soufi Y, Hashemnia MN. (2017). Fuzzy logic field oriented control of double star induction motor drive. Electrical Engineering 99: 495-503. https://doi.org/10.1007/s00202-016-0377-2

[13] Amimeur H, Aouzellag D, Abdessemedn R, Ghedamsi K. (2012). Sliding mode control of a dual-stator induction generator for wind energy conversion systems. International Journal of Electrical Power & Energy Systems 42: 60-70. https://doi.org/10.1016/j.ijepes.2012.03.024

[14] Rahali H, Zeghlache S, Benalia L. (2017). Adaptive field-oriented control using supervisory type-2 fuzzy control for dual star induction machine. International Journal of Intelligent Engineering and Systems 10(4): 28-40.

[15] Radwan TS. (2005). Perfect speed tracking of directe torque controlled induction motor drive using Fuzzy logic. International Conference Power Electronics and Drives Systems, PEDS, IEEE, Kuala Lumpur, Malaysia 38-43. https://doi.org/10.1109/PEDS.2005.1619657

[16] Loukal K, Benalia L. (2016). Interval type-2 fuzzy gain-adaptive controller of a doubly fed induction machine (DFIM). Journal of Fundamental and Applied Sciences 8: 470-493.

[17] Gao W, Hung JC. (1993). Variable structure control of nonlinear systems: A new approach. Electrical Engineering 40: 45-50. https://doi.org/10.1109/41.184820

[18] Zeghlache S, Kara K, Saigaa D. (2015). Fault tolerant control based on interval type-2 fuzzy sliding mode controller for coaxial trirotor aircraft. ISA Transactions 59: 215-231. https://doi.org/10.1016/j.isatra.2015.09.006

[19] Bouadi H, Bouchoucha M, Tadjine M. (2007). Sliding mode control based on backstepping approach for an UAV type-quadrotor. World Academy of Science, Engineering and Technology 26: 22-27.

APPENDIX A

Nomenclature of the parameters DSIM model.

$V_{ds}, V_{qs} V_{dr}$, V_{qr}	Stator and rotor voltages d-q axis components
i_{ds} , i_{qs}, i_{dr}, i_{qr}	Stator and rotor currents d-q axis components
φ_s, φ_r	stator - rotor flux
φ_d, φ_q	Stator flux d- q axis components
ω_s, ω_r	stator and rotor pulsation respectively
ω_{sref}, ω_{rref}	Stator and rotor pulsation references respectively
φ_{rref}	rotor flux control reference
R_s , R_r	Stator- Rotor resistance
T_r	Load torque
ω	Mechanical speed
ω_{glref}	Sliding speed reference
C_{em}	Electromagnetic torque
L_s , L_r	Stator- and Rotor inductance respectively

L_m	Mutual inductance
J	Total inertia
p	Number of pole pairs
K_f	Friction coefficient

APPENDIX B

DSIM motor parameters.

Item	Symbol	Data
DSIM Mechanical Power	P_w	*4.5 kW*
Nominal Voltage	V_n	*220 V*
Nominal Current	I_n	*6.5 A*
Nominal speed	ω_n	*300 rad/s*
Pole pairs number	p	*1*
Stators resistances	$R_{s1} = R_{s2}$	*3.72 Ω*
rotor resistance	R_r	*2.12 Ω*
Stators self inductances	$L_{s1} = L_{s2}$	*0.22 H*
rotor self inductance	L_r	*0.006 H*
mutual inductance	L_m	*0.3672 H*
Moment of inertia	J	*0.625 kg.m²*
friction coefficient	K_f	*0.001Nms/rad*
Nominal Frequency	f	*50 Hz*